Rev. Adv. Mater. Sci. 31 (2012) 5-11

PROCESSING SHEETS AND WIRES BY CONTINUOUS HIGH-PRESSURE TORSION

Kaveh Edalati[1,2] and Zenji Horita[1,2]

[1]Department of Materials Science and Engineering, Faculty of Engineering, Kyushu University, Fukuoka 819-0395, Japan
[2]WPI, International Institute for Carbon-Neutral Energy Research (WPI-I2CNER), Kyushu University, Fukuoka 819-0395, Japan

Received: April 20, 2012

Abstract. Continuous high-pressure torsion (HPT) method was applied to pure Al (99.99%) and an Al–3%Mg–0.2%Sc alloy. It is shown that continuous HPT (CHPT) can be used for severe plastic deformation and thus for production of ultrafine grained microstructure as the conventional HPT. Furthermore, CHPT provides a means to process sheet and wire of the materials in a continuous way so that it can be promising for industrial applications. It is confirmed that an Al-3%Mg-0.2%Sc alloy exhibits superplastic elongation of ~500% at 573K after processing by the CHPT.

1. INTRODUCTION

Processing bulk metallic materials through the application of severe plastic deformation (SPD) leads to attainment of ultrafine-grained structures with a high strength and reasonable ductility [1-3]. Among different SPD methods, high-pressure torsion (HPT), in which a disc or ring is subjected to high pressure and simultaneous torsional straining [4], has capability of continuously imposing extremely large shear strains up to a steady-state (saturation) level [5,6].

So far, HPT has been successfully applied to a wide range of materials such as metallic materials (e.g., [7-13]), semi-metals (e.g., [14,15]), intermetallics (e.g., [16,17]), amorphous materials (e.g., [18,19]) and ceramics [20,21]. In addition to the grain refinement and resultant physical and mechanical properties, HPT provides unique opportunity for consolidation of metallic powders [22,23], amorphous materials [18,19], ceramics [20,21] and machining chips [24-26]. The method is also applicable for controlling the allotropic phase transformations in several materials such as Ti [27-29], Zr [30-32], and ZrO_2 [21] as well as for decomposition of supersaturated solid soluted alloys such as Al-Zn [33], Al-Mg [33], and Co-Cu [34].

Despite these merits of HPT, the technique is not potential for industrial applications because of two reasons: first, the method is used in a form of disc [7-36] or ring [37,38] specimens which have restricted applications in the industry when compared to sheets or wires, and second, the dimensions of samples are so small (maximum 40 mm diameter for discs [6] and 100 mm diameter for rings [37]). Continuous HPT (CHPT), which is schematically illustrated in Fig. 1, was recently developed for processing of long lengths of sheets [39] and wires [40] of pure metals. The method was also conducted using sheets of an Al–3%Mg–0.2%Sc alloy [41] which is known to exhibit superplasticity if the alloy is processed by SPD to refine the grain size to the submicrometer level [42-44].

In this paper, thus, we review our recent studies on the development of CHPT for practical use of HPT to produce ultrafine-grained sheets and wires.

Corresponding author: Kaveh Edalati, e-mail: kaveh.edalati@zaiko6.zaiko.kyushu-u.ac.jp

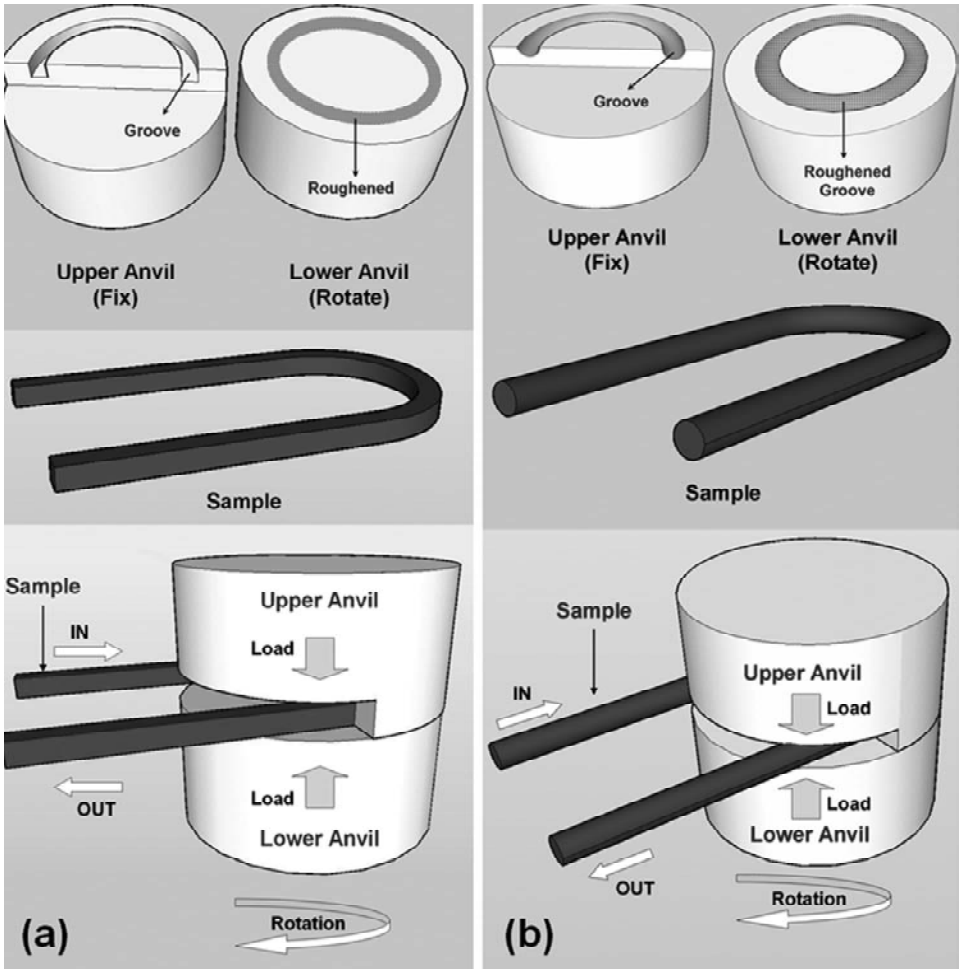

Fig. 1. Schematic illustration of CHPT using (a) sheets [37] and (b) wires [38].

Summary of recent study is first given including examination of hardness, tensile properties and microstructures. This is then followed by requirements for future developments of the continuous processing of HPT.

2. EXPERIMENTAL PROCEDURES

The experiments were conducted using sheets of high-purity Al (99.99%) and an Al–3%Mg–0.2%Sc alloy (in wt.%). Sheets of the pure Al and alloy were cut to U-shaped specimens having 1 mm thickness, 3 mm width, and 80 mm length including a half circle with outer diameter of *OD* = 20 or 30 mm. Wires of pure Al (99.99%) with 2 mm diameter were also used for the experiments. The wires were bent to U-shape with outer diameter of *OD* = 40 mm. The Al sheets were annealed for 1 hour at 773K, the Al–3%Mg–0.2%Sc alloy was solution treated in air for 1 hour at 873K before HPT processing, and the Al wires were used in an as-drawn form. The grain size of Al was 1050 μm after annealing and the grain size of the Al–3%Mg–0.2%Sc alloy was 400 μm after solution treatment.

The facility for the CHPT consists of two anvils. The lower anvil, which is rotated during process, has a flat surface with a roughened ring-shaped area for processing of sheets (Fig. 1a) and a roughened ring-shaped groove with circular cross sections of 2 mm diameter, 0.9 mm depth and outer diameter of *OD* = 40 mm for processing of wires (Fig. 1b). The upper anvil, which is fixed during process, has a half ring-shaped groove on the surfaces with 0.5 mm depth, 3 mm width and outer diameter of *OD* = 20 or 30 mm for processing of sheets and a half ring-shaped groove with circular cross sections with 2 mm diameter, 0.9 mm depth and outer diameter of *OD* = 40 mm for processing of wires.

A U-shaped specimen is placed on the lower anvil and a pressure of 1 GPa for Al and 1.25 GPa for the alloy is applied on the sample by raising the lower anvil up to a rigid contact with the upper anvil. The lower anvil is then rotated with respect to the upper anvil for either 1/4, 1 or 2 revolutions. Accord-

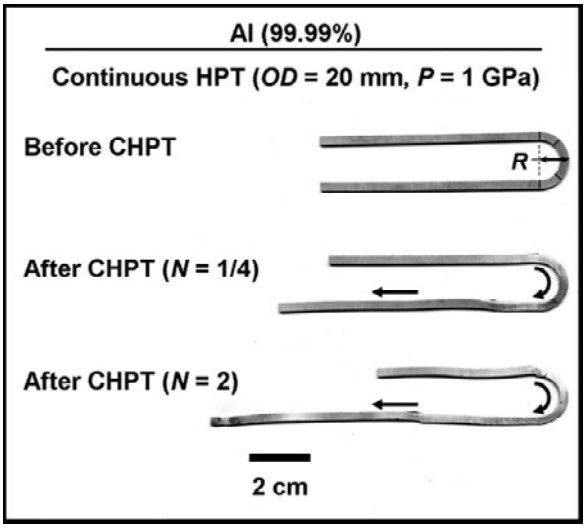

Fig. 2. Appearance of U-shaped Al sheet samples with before and after CHPT for 1/4 and 2 revolutions.

ingly the material starts to flow in the rotation direction. Fig. 2 shows the appearance of Al sheet samples before and after CHPT for 1/4 and 2 revolutions.

The equivalent strain produced by CHPT, ε, is given as [39]

$$\varepsilon = (1-s)\frac{\pi R}{\sqrt{3}\,t}, \qquad (1)$$

where s is the fraction of sample slippage as described in an earlier report [45], R is the mean radius of the U-shaped sample and t is the thickness of sample. Since s is estimated in the range of $0 < s < 1/2$ in earlier papers [39,40], here, the equivalent strain was estimated under the condition of $s = 1/4 \pm 1/4$.

The samples subjected to CHPT were evaluated in terms of Vickers microhardness, tensile properties and transmission electron microscopy (TEM).

First, the sheet and wire samples were polished to a mirror-like surface and the Vickers microhardness was measured at 5 mm away from the exit of the upper anvil. For each hardness measurement, a load of 50 g for Al and a load of 200 g for Al–3%Mg–0.2%Sc were applied for 15 seconds and the average of hardness values was calculated.

Second, miniature tensile specimens having 1 mm gauge length and 1mm gauge width were cut from the Al–3%Mg–0.2%Sc samples in the direction parallel to the longitudinal axis of the sheet using a wire-cutting electric discharge machine. Each tensile specimen was mounted horizontally on grips and pulled to failure using a tensile testing machine with an initial strain rate of 3.3×10^{-3} s^{-1} at 573K and the stress-strain curve was delineated for each specimen.

Third, discs with 3 mm in diameter and rectangular chips with dimensions of $0.15\times2\times3$ mm^3 were prepared from the positions 5 mm away from the exit of the upper anvil. The discs and chips were ground mechanically to a thickness of 0.15 mm and further polished with an electro-chemical polisher using the solution given in Refs. [39,40,44]. TEM was performed at a voltage of 200 kV for microstructural observation and for recording selected-area electron diffraction (SAED) patterns.

3. RESULTS

The average of hardness values was taken for each sample and plotted in Fig. 3 together with earlier data obtained by conventional HPT of Al (99.99%) using disc specimens [8]. It is apparent that the hardness values for the sheet and wire samples processed by CHPT lie well on the steady-state (saturated) level obtained for disc samples after processing with HPT, although the hardness level for wire sample processed by CHPT is slightly higher than the steady-state level. It is noted that the measurement error of the hardness is within the symbols for the sheet and wire CHPT. Earlier papers found that the results of hardness measurements for Cu and Fe after CHPT are consistent with those of conventional HPT using disc and ring specimens and hardness reaches the steady-state levels just after one pass through the anvils [39,40].

TEM bright-field image, SAED pattern and dark-field image are shown in Figs. 4a-4c for the Al wires subjected to CHPT. Note that the dark-field image was taken with the diffracted beam indicated by the arrow in the SAED pattern. Inspection of Fig. 4a reveals that few dislocations are visible in the grains and that grain boundaries are straight and well defined with an average grain size of ~1.3 μm. These microstructural features are consistent with earlier observations using conventional HPT [37-40]. Moreover, several elongated grains are seen in Fig. 4c, and this is different from equiaxed grain features observed earlier using the conventional HPT [37-40]. The configuration of the elongated grains may be attributed to a strong directional flow of material during CHPT or to the relatively thick and round cross section for the wire sample. The earlier experiments found that ultrafine-grained microstructures are achieved successfully in Cu and Fe after processing by CHPT [39].

The hardness for the Al–3%Mg–0.2%Sc alloy sheet after processing by CHPT is plotted in Fig. 5

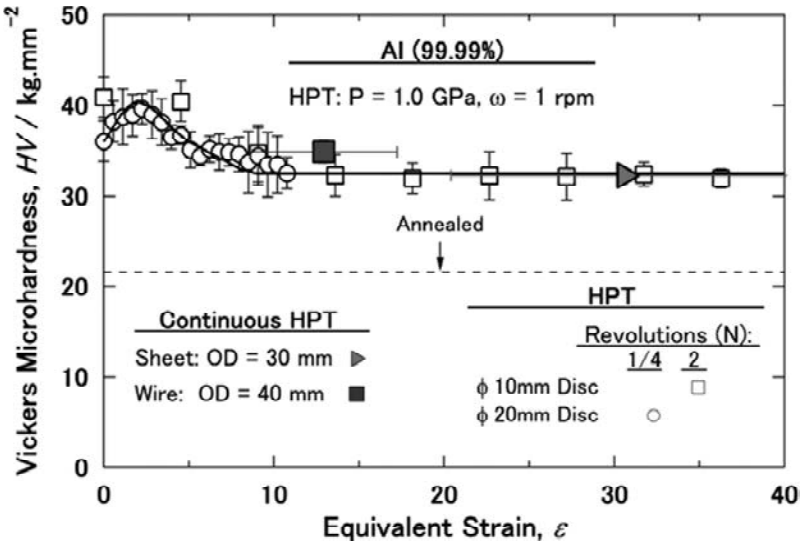

Fig. 3. Hardness value for CHPT using sheet and wire samples plotted against equivalent strain in graph reported earlier using conventional HPT for disc specimens of Al [35].

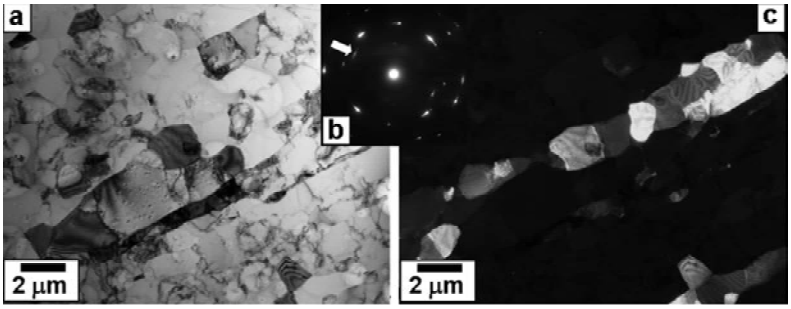

Fig. 4. TEM (a) bright-field and (b) dark-field micrographs including (c) SAED pattern of an Al wire after processing with CHPT.

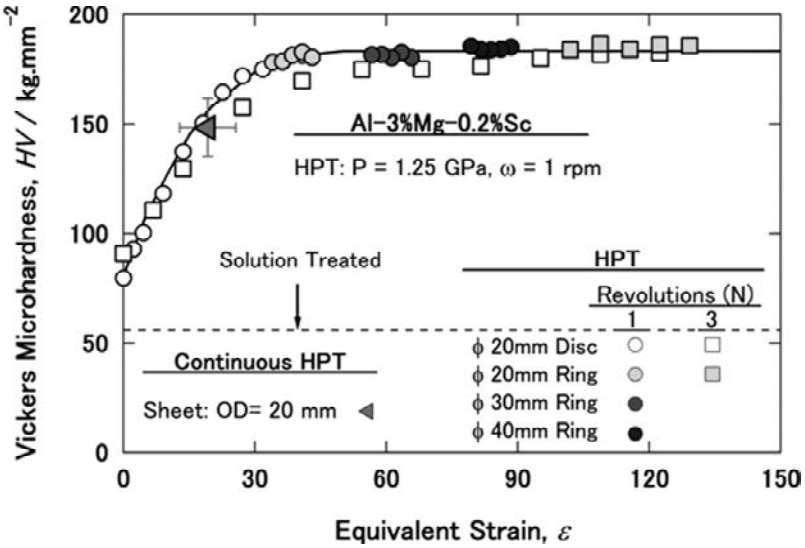

Fig. 5. Hardness value for CHPT using sheet sample plotted against equivalent strain in graph reported earlier using conventional HPT for disc and ring specimens of Al-3%Mg-0.2%Sc [40].

together with earlier data obtained by conventional HPT using disc and ring specimens [43]. The present results of CHPT are reasonably consistent with those of HPT-processed disc and ring samples [42,43]. It is found that the hardness value for CHPT is still in the level before reaching the saturation. Since the equivalent strain is insufficient to reach the steady state, this low level of hardness is reasonable.

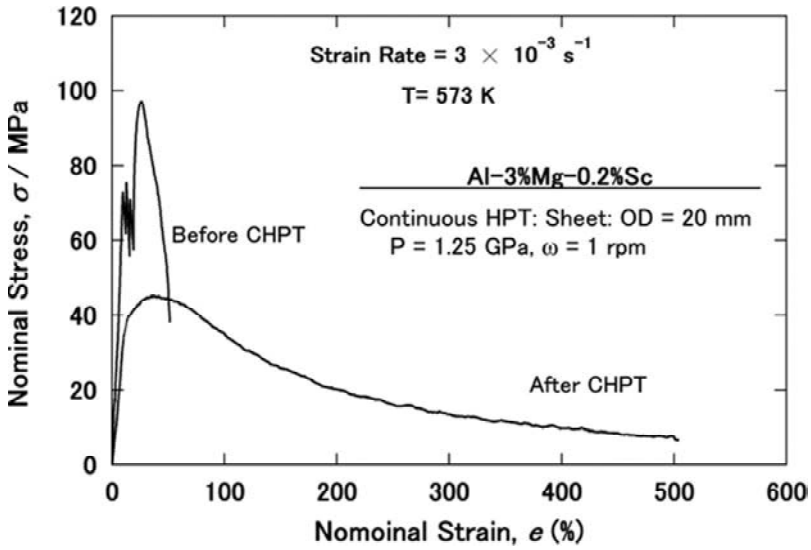

Fig. 6. Nominal stress versus nominal strain curves of Al-3%Mg-0.2%Sc sheet before and after processing by CHPT.

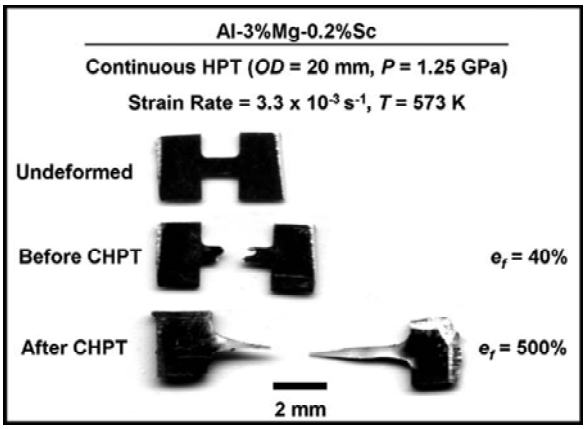

Fig. 7. Appearance of tensile specimens of Al-3%Mg-0.2%Sc sheet after pulling to failure at 573K before and after processing by CHPT. Undeformed specimen is also included.

The stress-strain curves are shown in Fig. 6 from tensile testing conducted at 573K at an initial strain rate of 3.3×10^{-3} s^{-1} for the alloy before and after processing with CHPT. Following the CHPT, the tensile strength decreases from 96 to 45 MPa and the total elongation to failure increases from ~40% to ~500%. It is confirmed that a superplastic elongation of ~500% is obtained by processing with CHPT. However, this elongation is insufficient when compared with 1510% reported earlier for processing with conventional HPT [43]. The difference can be attributed to the fact that less strain is introduced as shown in Fig. 6 and thus full development of an ultrafine-grained microstructure is not attained. The appearance of the tensile specimens before and after testing is shown in Fig. 7. It is demonstrated that processing by CHPT leads to the advent of superplasticity at 573K. It is noted that serration appears on the sample before processing by CHPT but not on the sample after the CHPT. This can be attributed to the effect of solute atoms on dynamic strain hardening behavior and Portevin–LeChatelier instability as often observed in solid-solution hardening alloys like Al-3%Mg [46]. For the CHPT-processed sample, the Portevin–LeChatelier instability becomes insignificant because of grain refinement as shown in Ref. [42-44]. The decomposition of supersaturated solid solution as reported in Ref. [33] may also affect the Portevin–LeChatelier instability.

4. DISCUSSIONS

Several important points should be considered for future developments of CHPT method.

First, although the slippage between the anvils and the sample is undesired in conventional HPT [5,45], a continuous flow of the material in the rotation direction is enabled by the slippage in CHPT. In order to optimize the slippage and have a continuous flow of the materials, the surface roughness of the groove on the upper anvil is intentionally reduced with respect to the surface roughness of the groove on the lower anvil in CHPT [39,40].

Second, one important advantage of CHPT when compared to other continuous SPD methods is that a steady-state of hardness and a minimum grain size is reached just after one pass through the anvils. However, other continuous SPD methods, the workpiece should be subjected to several repetitive passes to attain high strains and reach the steady levels [47,48]. The sample state can be checked easily whether it is in the steady-state level or not

with reference to the plot of hardness versus equivalent strain as shown in Fig. 3 and Fig. 5.

Third, the strain imparted by HPT can be estimated with the three main parameters such as the distance from the disc or ring center, the rotation angle and the sample thickness for the HPT process. In association with this point, the diameter of groove on the anvils should be increased for processing thicker sheets or wires to impose a higher level of strain (see Eq. 1). It is noted that both imposed strain and processing speed are increased as the ring diameter increases and this can be met more with a practical requirement.

Forth, although the samples of pure metals with lengths of 100 mm was processed by CHPT in this study, this length can be increased easily by using proper feeding guides.

Fifth, the sheet or wire should be drawn to slightly an upward direction and pulled out in tension using proper guides to keep the material flow continuous.

Sixth, the sheet and wire samples are twisted during the process, and thus, subsequent shaping processes may be required to modify the shape of the samples such as rolling for the sheets and wire drawing or round-concave rolling for the wires.

Seventh, CHPT was operated properly in this study despite the unsymmetrical geometry between the upper and lower anvils as illustrated in Fig. 1. However, they should be symmetrical to avoid any unexpected breaking of the sheets and wires for continuous smooth operation. In order to make the pressure center coincident with the rotation axis of the anvils and thus keep the alignment between the upper anvil and the lower anvil best, it is suggested to have a supporter on the other half of the upper anvil or to introduce a two-way feeding system around the rotational axis.

Eighth, on the contrary to pure metals, the Al–3%Mg–0.2%Sc sheet samples broke after ~1/4 revolutions in this study. This can be due mostly to a low ductility of the alloy at room temperature after processing by SPD. However, the processing for less ductile materials can be circumvented by increasing the operation temperature. HPT operation at elevated temperature is feasible as the system can easily accommodate the direct heating of the sample [49].

5. CONCLUSIONS

Continuous high-pressure torsion (HPT) was applied to sheets and/or wires of high purity Al and an Al–3%Mg–0.2%Sc alloy. The results confirmed that processing by continuous HPT (CHPT) is effective in producing ultrafine grains and subsequent enhancement of hardness in metals and the Al–3%Mg–0.2%Sc alloy. The advent of superplasticity in the Al–3%Mg–0.2%Sc alloy was also confirmed as by the conventional HPT. It is concluded that HPT can be operated continuously to produce sheets and wires having ultrafine grained structures and enhanced mechanical properties and, therefore, the CHPT introduced in this study provides a good potential for practical application of the HPT processing.

ACKNOWLEDGEMENTS

One of the authors (KE) would like to thank the Islamic Development Bank (IDB) for a doctoral scholarship and Japan Society for Promotion of Science (JSPS) for a postdoctoral scholarship. This work was supported in part by the Light Metals Educational Foundation of Japan, in part by a Grant-in-Aid for Scientific Research from the MEXT, Japan, in Innovative Areas “Bulk Nanostructured Metals” and in part by Kyushu University Interdisciplinary Programs in Education and Projects in Research Development (P&P).

REFERENCES

[1] R.Z. Valiev, R.K. Islamgaliev and I.V. Alexandrov // *Prog. Mater. Sci.* **45** (2000) 103.
[2] R.Z. Valiev, I.V. Alexandrov, Y. T. Zhu and T.C. Lowe // *J. Mater. Res.* **17** (2002) 5.
[3] R.Z. Valiev, Y. Estrin, Z. Horita, T.G. Langdon, M.J. Zehetbauer and Y.T. Zhu // *JOM* **58 (4)** (2006) 33.
[4] P.W. Bridgman // *Phys. Rev.* **48** (1935) 825.
[5] A.P. Zhilyaev and T.G. Langdon // *Prog. Mater. Sci.* **53** (2008) 893.
[6] R. Pippan, S. Scheriau, A. Taylor, M. Hafok, A. Hohenwarter and A. Bachmaier // *Annu. Rev. Mater. Res.* **40** (2010) 319.
[7] H.S. Kim, S.I. Hong, Y.S. Lee, A.A. Dubravina and I.V. Alexandrov // *J. Mater. Proc. Technol.* **142** (2003) 334.
[8] Y.H. Zhao, J.F. Bingert, X.Z. Liao, B.Z. Cui, K. Han, A.V. Sergueeva, A.K. Mukherjee, R.Z. Valiev, T. G. Langdon and Y.T. Zhu // *Adv. Mater*. **18** (2006) 2949.
[9] M. Kawasaki, B. Ahn and T.G. Langdon // *J. Mater. Sci.* **45** (2010) 4583.
[10] M. Zehetbauer, R. Grossinger, H. Krenn, M. Krystian, R. Pippan, P. Rogl, T. Waitz and R. Wurschum // *Adv. Eng. Mater.* **12** (2010) 692.

[11] A.P. Zhilyaev, S. Lee, G.V. Nurislamova, R.Z. Valiev and T.G. Langdon // *Scripta Mater.* **44** (2001) 2753.
[12] B.J. Bonarski, E. Schafler, B. Mingler, W. Skrotzki, B. Mikulowski and M.J. Zehetbauer // *J. Mater. Sci.* **43** (2008) 753.
[13] Y. Song, E.Y. Yoon, D.J. Lee, J.H. Lee and H.S. Kim // *Mater. Sci. Eng. A* **528** (2011) 4840.
[14] R.K. Islamgaliev, R. Kuzel, S.N. Mikov, A.V. Igo, J. Burianek, F. Chmelik and R.Z. Valiev // *Mater. Sci. Eng. A* **266** (1999) 205.
[15] K. Edalati and Z. Horita // *Scripta Mater*. **64** (2011) 161.
[16] J.Y. Huang, Y.T. Zhu, X.Z. Liao and R.Z. Valiev // *Phil. Mag. Lett*. **84** (2004) 183.
[17] C. Mangler, C. Gammer, H.P. Karnthaler and C. Rentenberger // *Acta Mater*. **58** (2010) 5631.
[18] A.R. Yavari, W.J. Botta, C.A.D. Rodrigues, C. Cardoso and R.Z. Valiev // *Scripta Mater*. **46** (2002) 711.
[19] J. Sort, D.C. Ile, A.P. Zhilyaev, A. Concustell, T. Czeppe, M. Stoica, S. Surinach, J. Eckert and M.D. Baro // *Scripta Mater*. **50** (2004) 1221.
[20] K. Edalati and Z. Horita // *Scripta Mater*. **63** (2010) 174.
[21] K. Edalati, S. Toh, Y. Ikoma and Z. Horita // *Scripta Mater.* **65** (2011) 974.
[22] I.V. Alexandrov, Y.T. Zhu, T.C. Lowe, R.K. Islamgaliev and R.Z. Valiev // *Metall. Mater. Trans. A* **29** (1998) 2253.
[23] A. Bachmaier, A. Hohenwartera and R. Pippan // *Scripta Mater*. **61** (2009) 1016.
[24] A.P. Zhilyaev, A.A. Gimazov, G.I. Raab and T.G. Langdon // *Mater. Sci. Eng. A* **486** (2008) 123.
[25] A.P. Zhilyaev, S. Swaminathan, A.A. Gimazov, T.R. McNelley and T.G. Langdon // *J. Mater. Sci*. **43** (2008) 7451.
[26] K. Edalati, Y. Yokoyama and Z. Horita // *Mater. Trans.* **51** (2010) 23.
[27] A.R. Kilmametov, A.V. Khristoforov, G. Wilde and R.Z. Valiev // *Z. Kristallogr. Suppl.* **26** (2007) 339.
[28] K. Edalati, E. Matsubara and Z. Horita // *Metall. Mater. Trans. A* **40** (2009) 2079.
[29] Y. Todaka, J. Sasaki, T. Moto and M. Umemoto // *Scripta Mater*. **59** (2008) 615.
[30] M.T. Perez-Prado, A.A. Gimazov, O.A. Ruano, M.E. Kassner and A.P. Zhilyaev // *Scripta Mater.* **58** (2008) 219.
[31] K. Edalati, Z. Horita, S. Yagi and E. Matsubara // *Mater. Sci. Eng. A* **523** (2009) 277.
[32] B. Srinivasarao, A.P. Zhilyaev and M.T. Perez-Prado // *Scripta Mater* **65** (2011) 241.
[33] B.B. Straumal, B. Baretzky, A.A. Mazilkin, F. Phillipp, O.A. Kogtenkova, M.N. Volkov and R.Z. Valiev // *Acta Mater* **52** (2004) 4469.
[34] B.B. Straumal, A.A. Mazilkin, B. Baretzky, G. Schutz, E. Rabkin and R.Z. Valiev // *Mater. Trans.* **53** (2012) 63.
[35] C. Xu, Z. Horita and T.G. Langdon // *Acta Mater*. **55** (2007) 203.
[36] M. Kawasaki, R.B. Figueiredo and T.G. Langdon // *Acta Mater*. **59** (2011) 308.
[37] K. Edalati and Z. Horita // *Mater. Trans*. **50** (2009) 92.
[38] Y. Harai, Y. Ito and Z. Horita // *Scripta Mater*. **58** (2008) 469.
[39] K. Edalati and Z. Horita // *J. Mater. Sci*. **45** (2010) 4578.
[40] K. Edalati, S. Lee and Z. Horita // *J. Mater. Sci*. **40** (2012) 473.
[41] K. Edalati and Z. Horita, In: *Proceedings of the 12th International Conference on Aluminum Alloys* (The Japan Institute of Light Metals: Yokohama, 2010), p. 1173.
[42] P.B. Berbon, S. Komura, A. Utsunomiya, Z. Horita, M. Furukawa, M. Nemoto and T.G. Langdon // *Mater. Trans. JIM* **40** (1999) 772.
[43] G. Sakai, Z. Horita and T. G. Langdon // *Mater. Sci. Eng. A* **393** (2005) 344.
[44] Y. Harai, K. Edalati, Z. Horita and T. Langdon // *Acta Mater.* **57** (2009) 1147.
[45] K. Edalati, Z. Horita and T. G. Langdon // *Scripta Mater*. **60** (2009) 9.
[46] J. Balik // *Mater. Sci. Eng. A* **316** (2001) 102.
[47] T.C. Lowe // *Mater. Sci. Forum* **667-669** (2011) 1145.
[48] R.Z. Valiev and T.G. Langdon // *Metall. Mater. Trans. A* **528** (2011) 6140.
[49] M. Kai, Z. Horita and T. G. Langdon // *Mater. Sci. Eng. A* **488** (2008) 117.